INTERNATIONAL BIWEEKLY ONLINE SEMINAR ON ANALYSIS, DIFFERENTIAL EQUATIONS AND MATHEMATICAL PHYSICS

Multiscale modeling of cardiovascular system

Sergey Simakov

simakovss@ya.ru

Department of Computational Physics, Moscow Institute of Physcis and Technology
Institue of Numerical Mathematics, Russian Academy of Sciences
Sechenov University

Motivation

- Cardiovascular diseases are the main reason of mortality and disability.
- Analysis of blood flow in the presence of stenosis, arrythmia, heart valve insufficieny, tumour angiogenesis is required.
- Mordern detailed models are difficult for implementation, patient-specific tuning and utilisation.
- Multiscale approach and computational tools for modelling haemodynamics in cardiovascular system with pathologies are required.

Aims & Scope

Multiscale approach and computational tools for modelling haemodynamics in cardiovascular system with pathologies are developed.

The models are based on

- physical pricniples
- accessible clinical data

and produce useful results for medical doctors.

Biological fluids

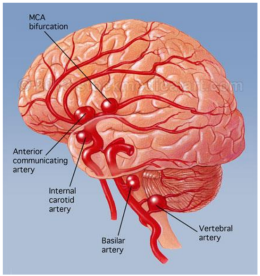

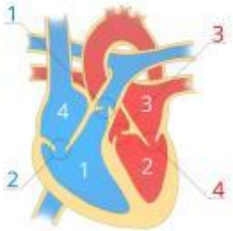

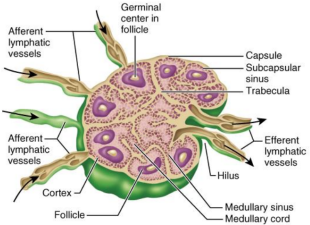

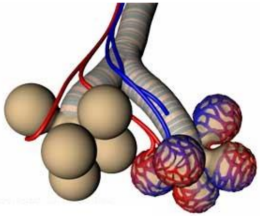

1D and 0D models

Figure: Heart chambers, aneurisms, lymphatic nodes, alveoli

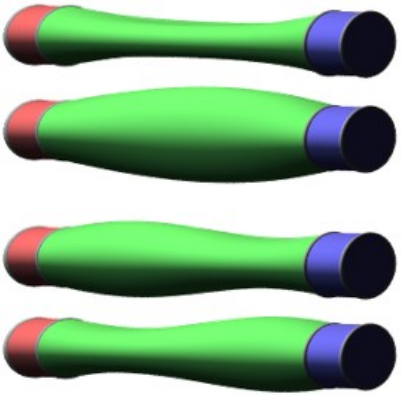

Figure: Arteries and veins, lymphatic vessels, bronchioles

1. Large arteries (3D, Dynamic)
   - Aorta
   - Carotid sinus
   - ...
2. Large and medium vessels ($L \gg d$) (1D, Dynamic)
   - Arteries
   - Superficial veins
   - Deep veins
   - Virtual (effective) vessels
3. Heart chambers, saccular aneurysm(0D, Dynamic)
4. Microcirculation (0D, Steady (stationary))

Conditions of hyperbolic formulation for 1D model of haemodynamics in a large vessel[1]

[1]Simakov S.S., Spatially averaged haemodynamic models for different parts of cardiovascular system, Russian Journal of Numerical Analysis and Mathematical Modelling, 2020, 35(5):285–294

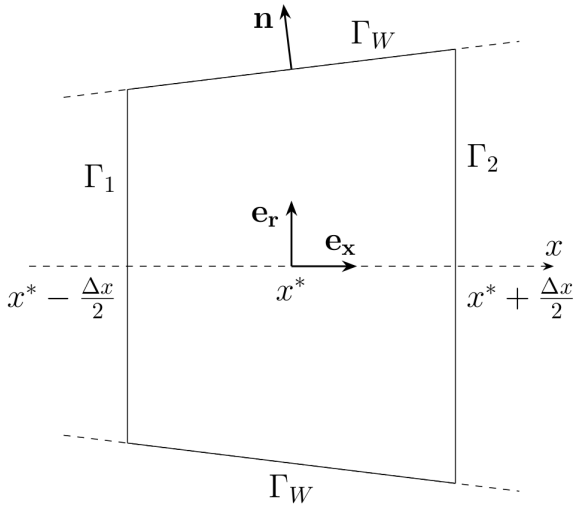
$\mathbf{n}$
Γ_W
Γ_1
Γ_2
$\mathbf{e_r}$
$\mathbf{e_x}$
x
$x^* - \frac{\Delta x}{2}$
x^*
$x^* + \frac{\Delta x}{2}$
Γ_W

$$\operatorname{div} \mathbf{u} = 0$$

$$\frac{\partial u_x}{\partial t} + \operatorname{div}\left(u_x \mathbf{u}\right) + \frac{1}{\rho}\frac{\partial P}{\partial x} - \nu \Delta u_x = 0$$

Assumptions:

$$u_x(t, x, y, z) = \bar{u}(t)\xi\left(x, y, z\right), u_r(t, R, x) = \frac{\partial \eta}{\partial t}(t, x)$$

$$\xi(x, y, z) = \frac{\gamma + 2}{\gamma}\left(1 - \left(\frac{y^2 + z^2}{R^2(t, x)}\right)^{\gamma/2}\right), \quad y^2 + z^2 \leqslant R^2(t, x)$$

$$u = \frac{1}{S}\int\limits_{\Gamma_S} u_x \, d\mathrm{s}, \quad Q|_{\Gamma_S} = \int\limits_{\Gamma_S} u_x \, d\mathrm{s} = Su$$

$$\frac{\partial S}{\partial t} + \frac{\partial Q}{\partial x} = 0$$

$$\frac{\partial Q}{\partial t} + \frac{\partial}{\partial x}\left(\alpha \frac{Q^2}{S}\right) + \frac{S}{\rho}\frac{\partial P}{\partial x} = K_r u$$

$$K_r = -2\pi\left(\gamma + 2\right)\nu, \quad \alpha = \frac{1}{Su^2}\int\limits_{\Gamma_S} u^2 \, d\mathrm{s} = \frac{\gamma + 2}{\gamma + 1}$$

$$\frac{\partial S}{\partial t} + \frac{\partial (Su)}{\partial x} = 0$$

$$\frac{\partial u}{\partial t} + \left(\alpha - \frac{1}{2}\right)\frac{\partial u^2}{\partial x} + (\alpha - 1)\frac{u^2}{S}\frac{\partial S}{\partial x} + \frac{1}{\rho}\frac{\partial P}{\partial x} = -2\pi(\gamma + 2)\nu\frac{u}{S}$$

$$P = F(S) \longrightarrow S = \hat{F}(P)$$

$$\frac{\partial F}{\partial S} > 0 \longrightarrow \frac{\partial \hat{F}}{\partial P} > 0$$

$$\frac{\partial u}{\partial t} + \left(\alpha - \frac{1}{2}\right)\frac{\partial u^2}{\partial x} + (1 + \varepsilon)\frac{1}{\rho}\frac{\partial P}{\partial x} = \psi(u, S)$$

$$\varepsilon = (\alpha - 1)\,\frac{\rho}{\rho_w}\,\frac{S_0}{S}\left(\frac{u}{c_0}\right)^2 \frac{1}{1 + \rho_w^{-1} c_0^{-2} P}$$

$$\gamma \geqslant 2 \longrightarrow 1 < \alpha = \frac{\gamma + 2}{\gamma + 1} \leqslant \frac{4}{3}$$

$$\left.\begin{aligned} &\rho < \rho_w \\ &S > S_0 \\ &u < 0.5\ m/s \\ &c_0 > 4\ m/s \end{aligned}\right\} \longrightarrow \varepsilon < 5 \cdot 10^{-3}$$

$$\frac{\partial u}{\partial t} + \frac{\partial}{\partial x}\left(\frac{u^2}{2} + \frac{P}{\rho}\right) = \psi$$

1D model of haemodynamics in a large vessel

$$\frac{\partial \mathbf{V}}{\partial t} + \frac{\partial \mathbf{F}\left(\mathbf{V}\right)}{\partial x} = \mathbf{G}\left(t, x, \mathbf{V}\right), \ \mathbf{V} = \begin{pmatrix} S \\ u \end{pmatrix}, \ \mathbf{F} = \begin{pmatrix} Su \\ \dfrac{u^2}{2} + \dfrac{P\left(t, S\right)}{\rho} \end{pmatrix}$$

Numerical discretisation

Internal nodes: explicit double-step conservative scheme[2]

$$\widehat{\mathbf{V}}_j = \mathbf{V}_j^n - \tau_{n+1}\left(\mathbf{F}_{j+1}^n - \mathbf{F}_{j-1}^n\right)/2h$$

$$\begin{aligned}\mathbf{V}_j^{n+1} =& \widehat{\mathbf{V}}_j + \left(\mathbf{\Omega}^{-1}\mathbf{B}\mathbf{\Omega}\right)_{j+1/2}\left(\mathbf{V}_{j+1}^n - \mathbf{V}_j^n\right) - \left(\mathbf{\Omega}^{-1}\mathbf{B}\mathbf{\Omega}\right)_{j-1/2}\left(\mathbf{V}_j^n - \mathbf{V}_{j-1}^n\right) + \\ &+ \left(\mathbf{\Omega}^{-1}\mathbf{D}\mathbf{\Omega}\right)_{j+1/2}\left(\widehat{\mathbf{V}}_{j+1} + \widehat{\mathbf{V}}_j - \mathbf{V}_{j+1}^n - \mathbf{V}_j^n\right) - \\ &- \left(\mathbf{\Omega}^{-1}\mathbf{D}\mathbf{\Omega}\right)_{j-1/2}\left(\widehat{\mathbf{V}}_j + \widehat{\mathbf{V}}_{j-1} - \mathbf{V}_j^n - \mathbf{V}_{j-1}^n\right) + \tau_{n+1}\mathbf{G}_j^n\end{aligned}$$

$$\mathbf{B}_{ij} = \{\delta_{ij}b_i\}, \mathbf{D}_{ij} = \{\delta_{ij}d_i\}, i = 1, 2$$

$$b_i = |\sigma_i|\left[1 + 5\left(1-\gamma\right)\left(1 - |\sigma_i|\right)/19\right]/2, \quad d_i = 6(1-\gamma)\sigma_i(1/|\sigma_i| - 1)/19, \sigma_i = \frac{\tau_{n+1}}{h}\left(\lambda_i\right)_j^n, \quad 0 \leqslant \gamma \leqslant 1$$

Stability: $|\sigma_i| < 1$, approximation: $\gamma = 0$ — second order

[2] Magomedov K.M., Kholodov A.S., Grid-characteristic numerical methods, Urait, 2017

Boundary conditions for smooth asymptotic solution in a vascular network

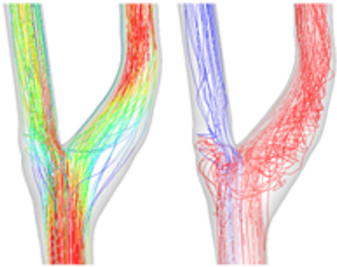

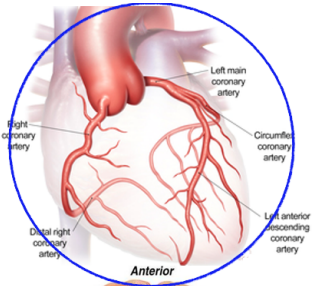
Left main coronary artery
Right coronary artery
Circumflex coronary artery
Distal right coronary artery
Left anterior descending coronary artery
Anterior

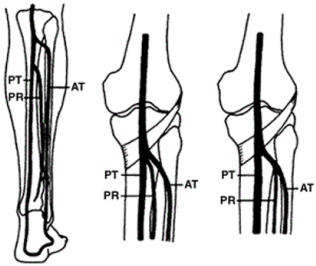
PT
PR
AT
PT
PR
AT
PT
PR
AT

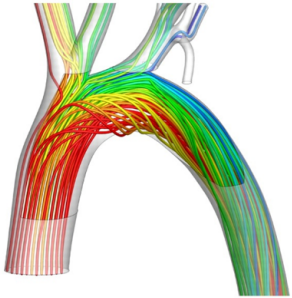

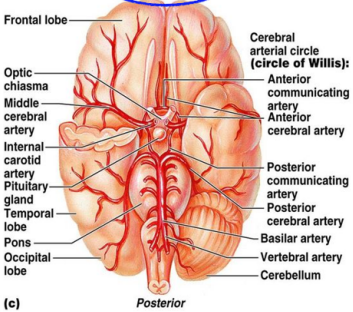
Frontal lobe
Optic chiasma
Middle cerebral artery
Internal carotid artery
Pituitary gland
Temporal lobe
Pons
Occipital lobe
Cerebral arterial circle (circle of Willis):
Anterior communicating artery
Anterior cerebral artery
Posterior communicating artery
Posterior cerebral artery
Basilar artery
Vertebral artery
Cerebellum
(c)
Posterior

1) Mass consevation

$$\sum_{k=k_1,k_2,\ldots,k_M} \varepsilon_k S_k\left(t,\tilde{x}_k\right) u_k\left(t,\tilde{x}_k\right) = 0, \varepsilon_k = \pm 1, \tilde{x}_k = 0 \text{ или } L_k$$

2) Compatibility conditions along outgoing characteristics

$$\omega_k \cdot \left(\frac{\partial \mathbf{V}_k}{\partial t} + \lambda_k \frac{\partial \mathbf{V}_k}{\partial x}\right) = \omega_k \cdot \mathbf{G}_k \quad \text{где} \quad \omega_k \frac{\partial \mathbf{F}_k}{\partial \mathbf{V}_k} = \lambda_k \omega_k$$

3) ... next slide $\longrightarrow$

3.1) For the arterial and venous connections

$$\frac{u_k^2\left(t,\tilde{x}_k\right)}{2}+\frac{P\left(S_k\left(t,\tilde{x}_k\right)\right)}{\rho}=I_M, k=k_1,\ldots,k_M$$

3.2) Arterio-venous connections (microcirculatory regions)

$$P_k\left(S_k\left(t,\tilde{x}_k\right)\right)-P_{node}\left(t\right)=\varepsilon_k R_k S_k\left(t,\tilde{x}_k\right)u_k\left(t,\tilde{x}_k\right), k=k_1,\ldots,k_M$$

3.3) Possible alternative for $Re\sim 1$

$$P_k\left(S_k\left(t,\tilde{x}_k\right)\right)=P_{node}, k=k_1,\ldots,k_M$$

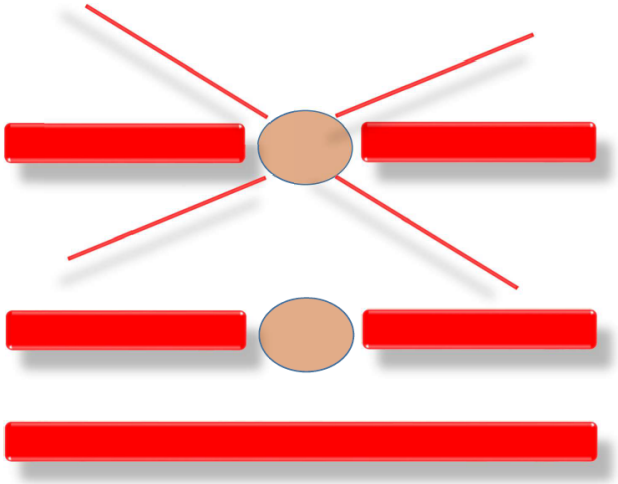

New boundary conditions [3]

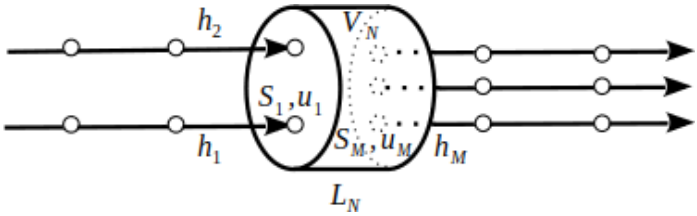

$$\Delta x \approx l, \quad V = lS$$

[3] Simakov S.S., New Boundary Conditions for One-Dimensional Network Models of Hemodynamics, Computational Mathematics and Mathematical Physics, 2021, 61(12): 2102–2117

$$\frac{dV_N}{dt} = \sum_{j=1}^{M} \varepsilon_j S_j u_j, j = 1, \dots M,$$

$$I_N \frac{d^2 V_N}{dt^2} + R_N \frac{dV_N}{dt} + P_{int} - P_{ext} = 0,$$

- P_{ext} — aveage pressure at the connections with incoming and outgoing vessels
- P_{int} — pressure in the junction due to the elasticity of the wall

$$P_{in}\left(V_N\right) = \frac{\sum\limits_{j=1}^{M} P_j\left(\frac{V_N}{L_N}\right)\left(S_0\right)_j^l}{\sum\limits_{j=1}^{M}\left(S_0\right)_j^l},$$

$$P_{ext}\left(S_1, S_2, ..., S_M\right) = \frac{\sum\limits_{j=1}^{M} P_j\left(S_j\right)\left(S_0\right)_j^l}{\sum\limits_{j=1}^{M}\left(S_0\right)_j^l}$$

$$L_N = \frac{\sum\limits_{j=1}^{M} h_j d_j}{\sum\limits_{j=1}^{M} d_j}, \quad V_N(0) = \frac{\sum\limits_{j=1}^{M} V_0 j \cdot \left(S_0\right)_j^l}{\sum\limits_{j=1}^{M}\left(S_0\right)_j^l}.$$

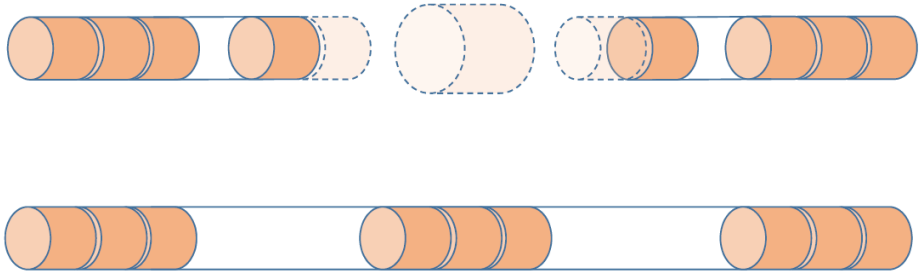

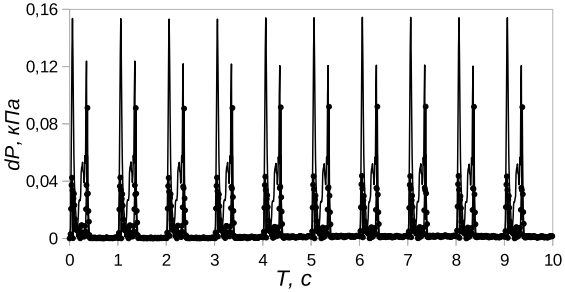

Figure: Absolute error of pressure in new model (marked) and Bernulli model (line without dots) at the center of the vessel.

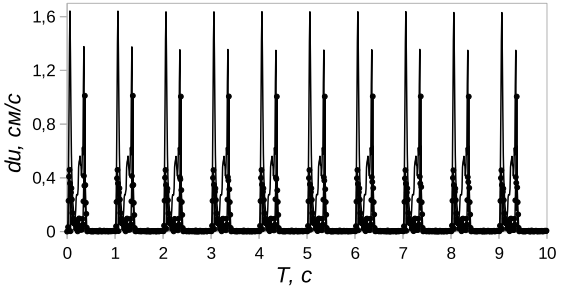

Figure: Absolute error of linear velocity in new model (marked) and Bernulli model (line without dots) at the center of the vessel.

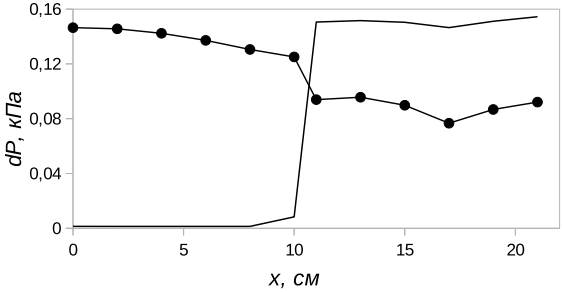

Figure: Maximum of the absolute error of pressure along the vessel in new model (marked) and Bernulli model (line without dots).

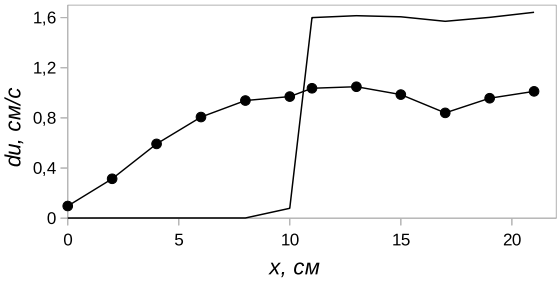

Figure: Maximum of the absolute error of linear velocity along the vessel in new model (marked) and Bernulli model (line without dots).

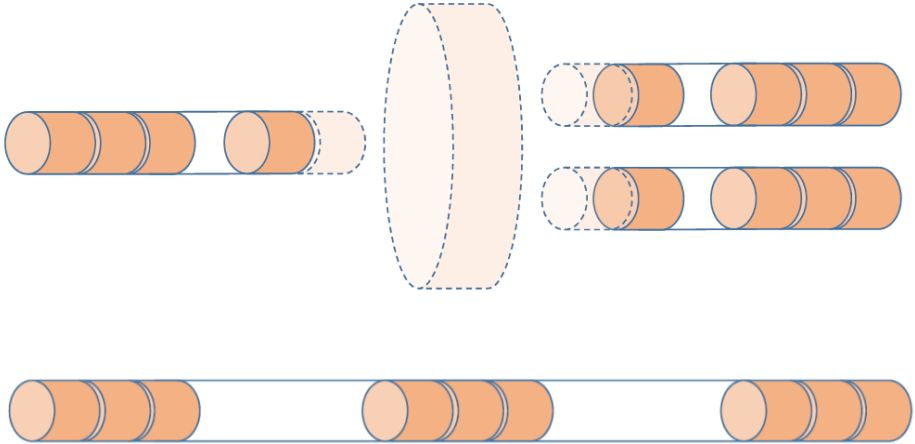

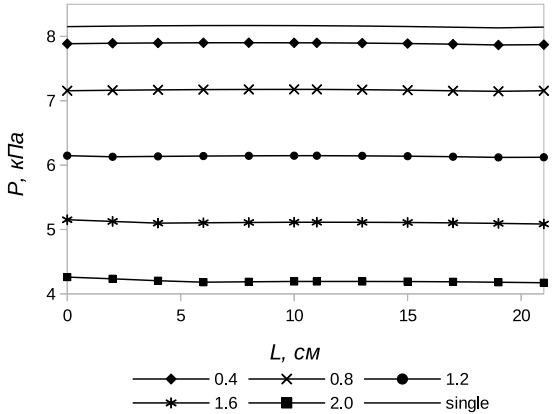

Figure: Systolic pressure along the major vessel depending on the diameter of the side branch.

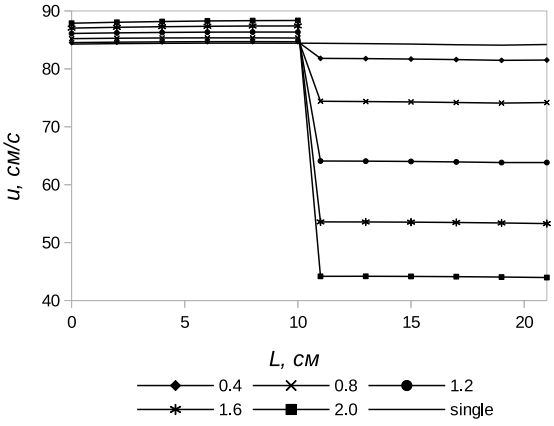

Figure: Systolic linear velocity along the major vessel depending on the diameter of the side branch.

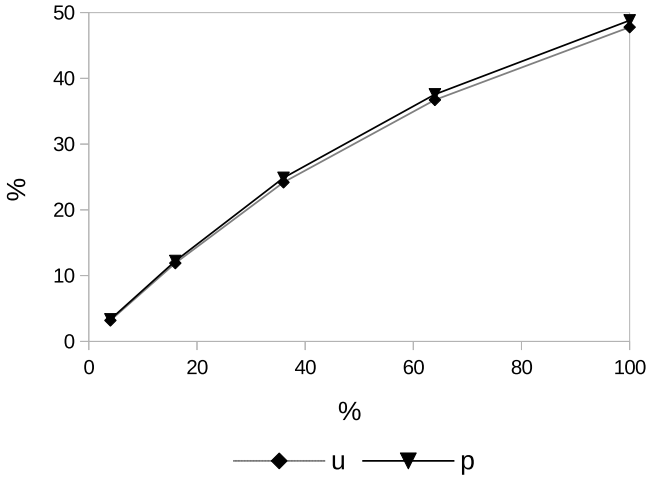

Figure: Systolic relative difference of linear velocity and pressure from the values in a single vessel depending on the relative area of the side branch.

Lumped parameter heart model with valve dynamics [4]

[4] Simakov S.S., Lumped Pparameter Heart Model with Valve Dynamics, Russian Journal of Numerical Analysis and Mathematical Modelling, 2019, 34(5):289–300

1
2
3
4
4
1
3
2

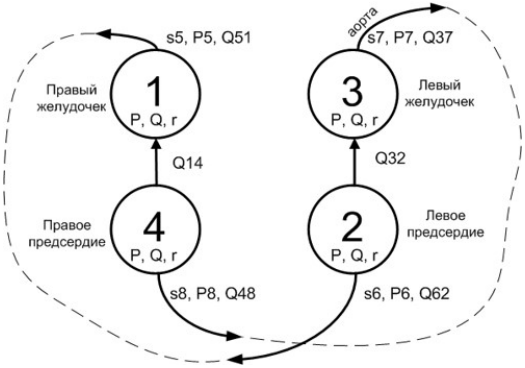
s5, P5, Q51
Правый желудочек
1
P, Q, r
Q14
Правое предсердие
4
P, Q, r
s8, P8, Q48
аорта
s7, P7, Q37
Левый желудочек
3
P, Q, r
Q32
Левое предсердие
2
P, Q, r
s6, P6, Q62

- Momentum conservation

$$\frac{\rho l^2}{V_j}\frac{d^2V_j}{dt^2} + 2\pi\nu\left(\gamma+2\right)\frac{\rho l^3}{V_j^2}\frac{dV_j}{dt} + e_j\left(t\right)\left(V_j - V_{j0}\right) = P_j, j = 1,\ldots,4$$

- Myocardium activation function

$$e_j\left(t\right) = E_j^{syst} + \frac{E_j^{syst} + E_j^{diast}}{2}e\left(t\right)$$

Boundary conditions

- Inter-chamber flows

$$Q_{ij} = \frac{\alpha_{ij}}{r_{ij}} (P_j - P_i)$$

- Mass conservation

$$\frac{dV_i}{dt} = \sum_j \alpha_{ij} Q_{ij}, i = 1, \ldots, 4,$$

α_{ij} — valve opening function

The valves are subjected by the friction force, pressure force and flow resistance force. The 2nd Newton's law can be stated as

$$\frac{d^2\theta_{ij}}{dt^2} = K^{fr}\frac{d\theta_{ij}}{dt} + K^p\left(P_j - P_i\right)\psi_{ij}\cos\theta_{ij} + F^r_{ij},$$

$$\psi_{ij} = \begin{cases} 0, P_i < P_j \text{ и } \theta_{ij} < \theta^{min}_{ij}, \\ 1, \text{ otherwise}, \end{cases}$$

$$F^r_{ij} = \begin{cases} 0, \theta^{max}_{ij}\theta_{ij} < \theta^{max}_{ij} \\ K^r \tan\left(10\left(\theta_{ij} - \theta^{max}_{ij}\right)\right), \theta_{ij} \geqslant \theta^{max}_{ij} \text{ и } \frac{d\theta_{ij}}{dt} > 0 \\ K^r \tan\left(10\left(\theta_{ij} - \theta^{min}_{ij}\right)\right), \theta_{ij} \leqslant \theta^{min}_{ij} \text{ и } \frac{d\theta_{ij}}{dt} < 0. \end{cases}$$

- Instant opening

$$\alpha_{ij} = \begin{cases} 0, 0 \leqslant t < T_{open,ij}, \\ 1, T_{open,ij} \leqslant t \leqslant T_{close,ij}, \\ 0, T_{close,ij} < t \leqslant T. \end{cases}$$

- Dynamics

$$\alpha_{ij} = \begin{cases} 0, -\infty < \theta \leqslant \theta_{ij}^{min}, \\ \dfrac{1 - \cos\theta_{ij}}{1 - \cos\theta_{ij}^{max}}, \theta_{ij}^{min} < \theta \leqslant \theta_{ij}^{max}, \\ 1, \theta > \theta_{ij}^{max} \end{cases}$$

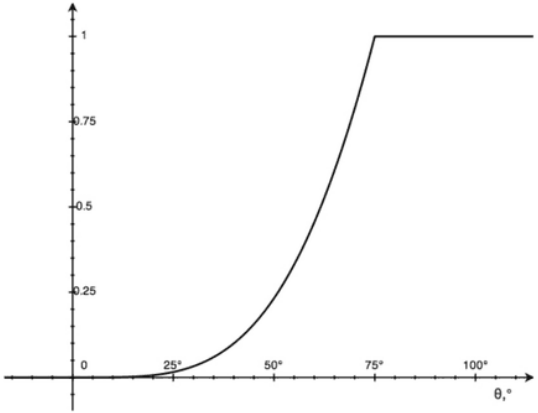

Figure: Valve function

Numerical discretisation: Obreshkov pairs method

$$\frac{d\vec{y}}{dt} = \vec{f}(t, \vec{y}) \to \frac{d\vec{y}}{dt} = \vec{w}, \frac{d\vec{w}}{dt} = \frac{\partial \vec{f}}{\partial t} + \frac{\partial \vec{f}}{\partial \vec{y}}\vec{y}$$

Implicit single-step Runge-Kutta method with Newton's method at each step

$$\vec{y}_{s+1}^{n+1} = \vec{y}_s^{n+1} - \mathbf{B}^{-1}\left(t^{n+1}, y^{n+1}\right)\vec{R}\left(\vec{y}_s^{n+1}\right), s = 1, 2, \ldots, \vec{y}_0^{n+1} = \vec{y}^n$$

$$\vec{R} = \sum_{k=0}^{1}\left[a_k\vec{y}^{n+k} - \tau b_k\vec{f}^{n+k} - \tau^2 c_k\left(\frac{\partial \vec{f}}{\partial t} + \frac{\partial \vec{f}}{\partial \vec{y}}\cdot\vec{y}\right)_{n+k}\right]$$

where

$$\mathbf{B} = \frac{\partial \vec{R}}{\partial \vec{y}^{n+1}} = \mathbf{E} - \tau b\frac{\partial \vec{f}}{\partial \vec{y}} - \tau^2 c\left(\frac{\partial}{\partial \vec{y}}\left(\frac{\partial \vec{f}}{\partial t}\right) + \left(\frac{\partial \vec{f}}{\partial \vec{y}}\right)^2 + \mathbf{C}\right), \mathbf{C} = \left\{\left(\frac{\partial}{\partial y_j}\left(\frac{\partial \vec{f}}{\partial \vec{y}}\right)\right)\cdot\vec{f}\right\}_j$$

Lumped model of microcirculation with tumour angiogenesis

Microvasculature

1. Generation of stochastic network (Validation: uiniform density distribution of capillaries side surface; volume ≈ 1 sm^3, number of the capillaries$\approx 10^5$)
2. Capillary flow computation (Validation: uniform density of the flow)

$$Q_{uv} = G_{uv}\left(P_v - P_u\right), \forall uv, \sum_{uv \in \mathcal{P}_u} Q_{uv} = 0, \forall u,$$

$$G_{uv} = \frac{8\mu l_{uv}}{\pi k_{uv} r_{uv}^4}(1 + \alpha Q_{uv}^2)^{-1}$$

Scheme of the network generation: first step

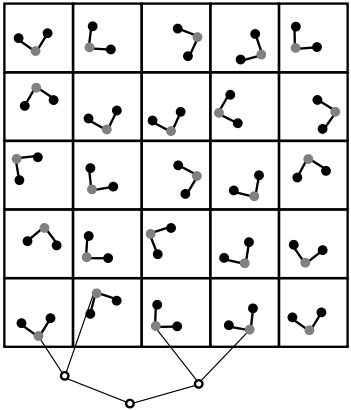

Validation by length statistics

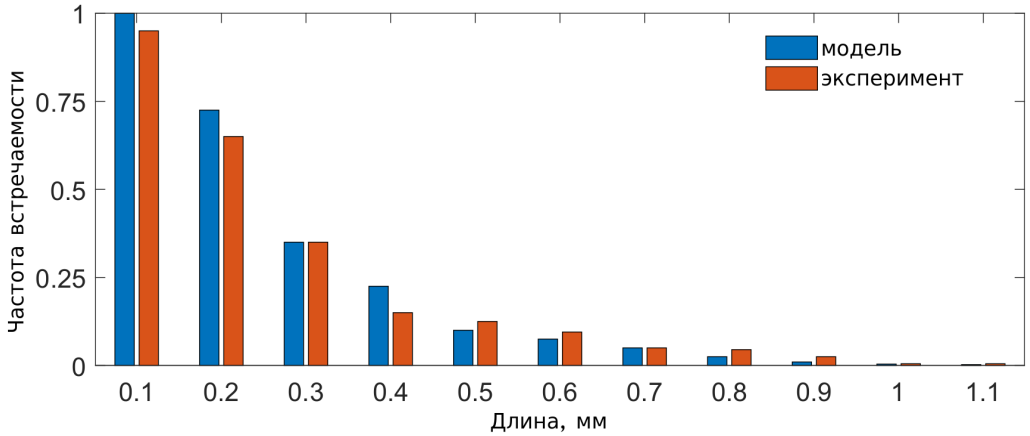

Modeling of haemodynamics for patients with cardiovascular pathologies

Coronary flow and variable heart rate [5]

[5] Gamilov T., ... Alastruey J., Simakov S. Computational analysis of coronary blood flow: The role of asynchronous pacing and arrhythmias, Mathematics, 2020, 8(8), 1205

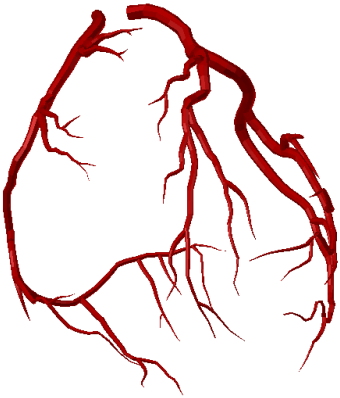

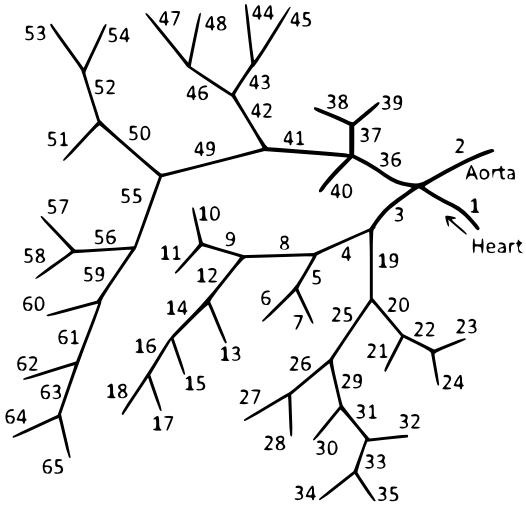
1
2
3
4
5
6
7
8
9
10
11
12
13
14
15
16
17
18
19
20
21
22
23
24
25
26
27
28
29
30
31
32
33
34
35
36
37
38
39
40
41
42
43
44
45
46
47
48
49
50
51
52
53
54
55
56
57
58
59
60
61
62
63
64
65
Aorta
Heart

Modified boundary conditinos

- Cardiac output

$$Q_H(t,\tau) = u(t,0)\,S(t,0)$$

$$Q_H(t,\tau) = \begin{cases} SV(\tau)\,\dfrac{\pi}{2\tau}\sin\left(\dfrac{\pi t}{\tau}\right), 0 \leqslant t \leqslant \tau \\ 0, \tau < t \leqslant T \end{cases}$$

$$SV(\tau) = 112[ml] - \frac{HR(\tau)\,[bpm]}{2[bpm/ml]}, \quad 40\ bpm < HR < 160\ bpm$$

$$\tau = 287.09[ms] - \frac{30685.24[ms^2]}{T[ms]},$$

$$\tau \text{ — systole duration}, \quad T[ms] = \frac{3600}{HR[bpm]}$$

- Outflow boundary conditions for terminal arteries

$$P_k\left(S_k\left(t,\tilde{x}_k\right)\right) - P_{veins} = R_k(t,\tau)S_k\left(t,\tilde{x}_k\right)u_k\left(t,\tilde{x}_k\right)$$

$$R_k\left(t,\tau\right) = \begin{cases} R_k + \left(R_k^{max} - R_k\right)\sin\left(\dfrac{\pi t}{\tau}\right), 0 \leqslant t \leqslant \tau, \\ R_k, \tau < t \leqslant T, \end{cases} \qquad R_k^{max} = 3R_k$$

Total systemic hydraulic resistance

$$R_{total} = \frac{\Delta P}{SV \cdot HR}, \quad \Delta P \approx 100 mmHg$$

1. Total coronary hydraulic resistance $\dfrac{R_{cor}}{R_{total}} = 5 \cdot 10^{-2}$ $\left(\dfrac{Q_{CBF}}{Q_{CO}} \approx 3 - 6\%\right)$
2. Murray's law in bifurcations $R_{RCA} \sim \left(d_{RCA}\right)^{2.27}, R_{LCA} \sim \left(d_{LCA}\right)^{2.27}$

Applications

- Asynchronous cardiac pacing of the LV and RV
- Tachycardia and bradycardia
- Long QT syndrome
- Premature ventricular contraction

Pacemaker placement

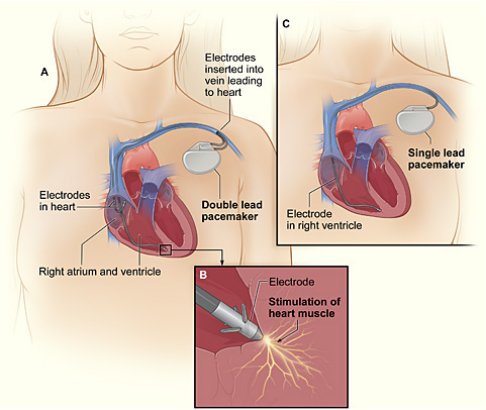

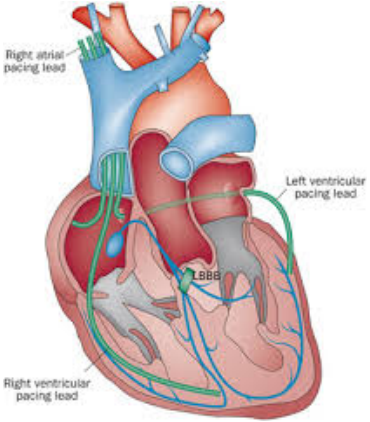

Asynchronous pacing

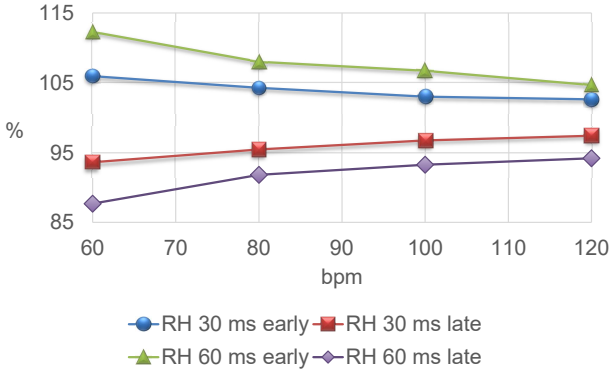

Average flow (relatve to the synchrounous pacing) in the right coronary artery for early (right ventricle stimulation) and late (left ventricle stimulation) right ventricle contraction

Tachycardia and bradicardia

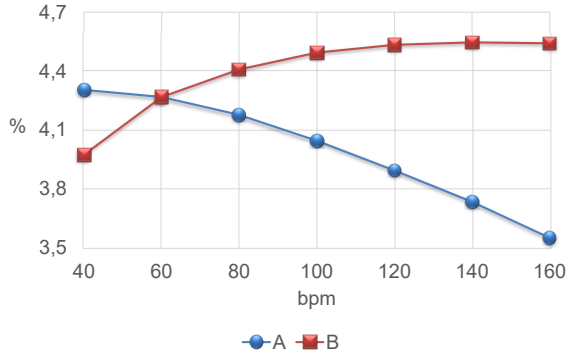

The fraction of coronary flow relative to the cardiac output
A — variable systole fraction, B — constant systole fraction (35%)

Tachycardia and bradicardia

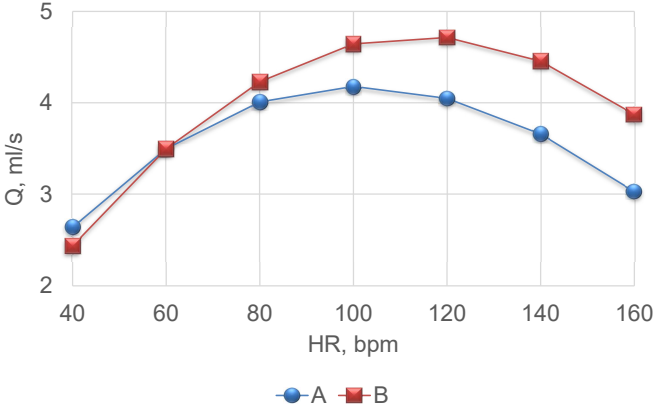

Coronary flow
A — variable systole fraction, B — constant systole fraction (35%)

Long QT syndrome: assumptions

- Long QT interval on ECG, which is more, than 480 ms, reflects the delay in myocardium repolarisation and myocardium relaxation after a heart contraction
- We set fraction of the systole to 49% regardless of HR
- We suppose, that SV and CO are not affected

Long QT syndrome: results

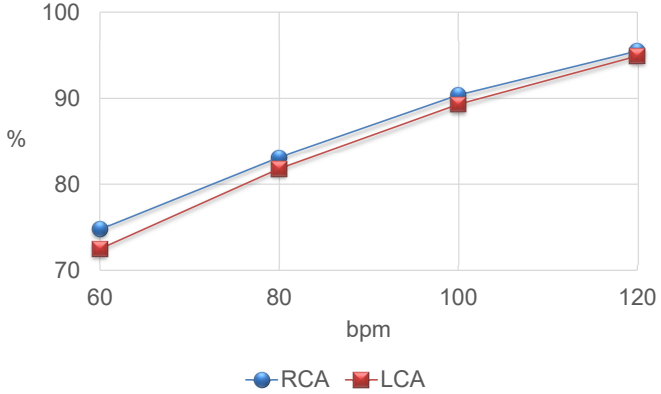

Flows in right (RCA) and left (LCA) coronary arteries

Premature ventricular contractions (PVC): assumptions

- Systole starts $0.25T$ earlier than a periodic schedule
- SV of the PVC is 71% less than SV of a normal beat due to insufficient ventricle filling
- The beat after PVC occurs on a schedule
- The total duration of PVC and the following beat is $2T$
- SV of the heartbeat after PVC is 18% more than SV of a normal beat due to increased ventricle filling

Premature ventricular contractions: assumptions

Bigeminy, trigeminy, quadrigeminy, ...

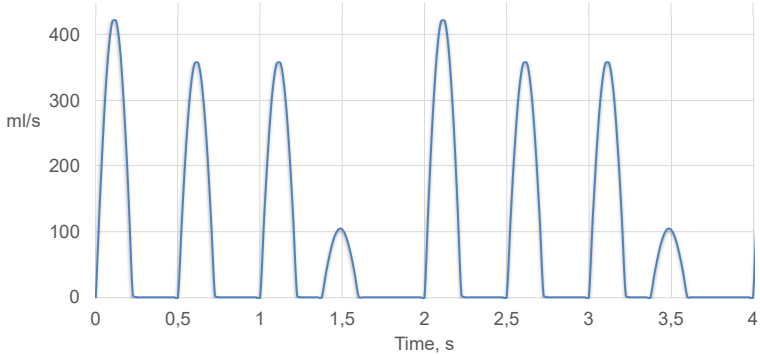

Modified output from left ventricle at 120 bpm and quadrigeminy

Premature ventricular contractions (PVC): results

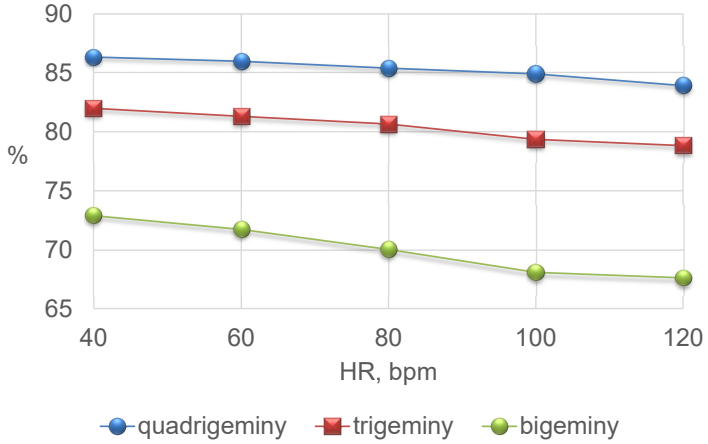

Coronary flow with PVC relative to the normal case

Cardiac output and insufficiency of the heart valves

Aortic regurgitation:

$$\theta_{ao}^{min} : 0^\circ \to 25^\circ$$

- Early aortic valve opening ($-0.05s/8.3\%$)
- Increase of the peak flow through the aortic valve up to 45%
- Backward flow through the aortic valve 70 ml/s
- Increase of the peak ventricule volume up to 30%

Mitral valve stenosis

$$\theta_{mi}^{max} : 75^\circ \to 50^\circ$$

- Late aortic valve opening ($+0.05s/8.3\%$)
- Deacrese of the peak area opening 25%
- Decrease of the peak flow through the arotic valve 40%
- Decrease of the peak flow through the mitral valve 75%
- Decrease of the peak ventricule volume to 25%
- Increase of the peak auricle volume up to 25%

Microcirculation with tumour angiogenesis

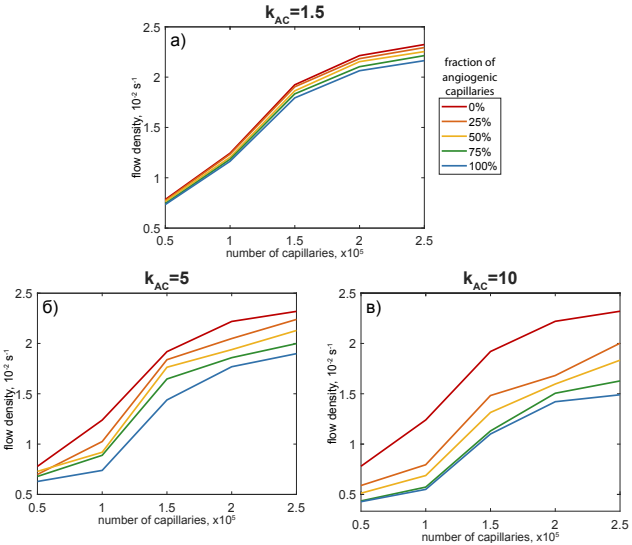

k_{AC} — ratio of the hydraulic resistances of agiogenic and preexisting capillaries

7

Patient-specific computational prediction of haemodynamics

MAGNETOM Espree

Patient

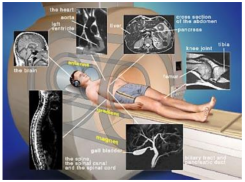

Diagnostics

Simulations

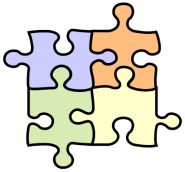

Frequent
(typical) cases

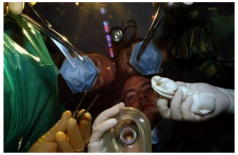

Prognosis, risk assessment,
recommendations, strategy, optimization

Coronary flow: Fractional flow reserve, arrhythmia

Cerebral flow, Carotid stenosis

Systemic arteries

Trasnport and metabolism: oxygen, carbon dioxide, drugs

LVAD

EECP

Venous reflux

Laparoscopic surgery

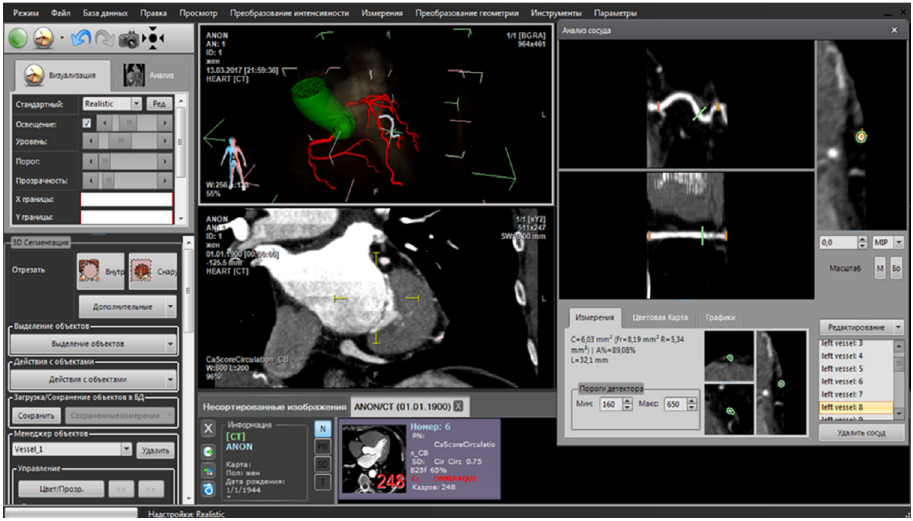
Режим
Файл
База данных
Правка
Просмотр
Преобразование интенсивности
Измерения
Преобразование геометрии
Инструменты
Параметры
Визуализация
Анализ
Стандартный:
Realistic
Ред.
Освещение:
Уровень:
Порог:
Прозрачность:
X границы:
Y границы:
3D Сегментация
Отрезать
Внутр
Снар
Дополнительные
Выделение объектов
Выделение объектов
Действия с объектами
Действия с объектами
Загрузка/Сохранение объектов в БД
Сохранить
Сохраненные измерения
Менеджер объектов
Vessel_1
Удалить
Управление
Цвет/Прозр.
ANON
AN: 1
ID: 1
жен
13.03.2017 [21:59:36]
HEART [CT]
1/1 [BGRA]
964x461
1/1 [sY2]
511x247
CaScoreCirculation_CB
W:500 L:200
96%
Несортированные изображения
ANON/CT (01.01.1900)
Информация
[CT]
ANON
Карта:
Пол: жен
Дата рождения:
1/1/1944
Номер: 6
PN:
CaScoreCirculatio
n_CB
SD: Cir Circ 0.75
825f 65%
OMNIPAQUE
Кадров: 248
Анализ сосуда
0,0
MIP
Масштаб
M
Бо
Измерения
Цветовая Карта
Графики
C=6,03 mm² (Fr=8,19 mm² R=5,34 mm²) | A%=89,08%
L=32,1 mm
Пороги детектора
Мин: 160
Макс: 650
Редактирование
left vessel: 3
left vessel: 4
left vessel: 5
left vessel: 6
left vessel: 7
left vessel: 8
Удалить сосуд
Надстройки: Realistic

Parameters identification

1. MRI/CT segmentation and anatomical structure production
2. Cardiac output
   - Heart rate variabliity [6]
   - Arterial pressure
   - Volume of the heart chambers
3. Terminal hydraulic resistances
   - Arterio-venous pressure difference
   - Flow distribution
4. Vascular stiffness (elasticity)
   - Age (stiffness increase), heght, sex, BMI, ...
   - Chronic diseases (hypertention, diabetes ...)
   - Life style (sport, smoking, alcohol, ...)

[6] already considered today

Fractional flow reserve (FFR) prediction

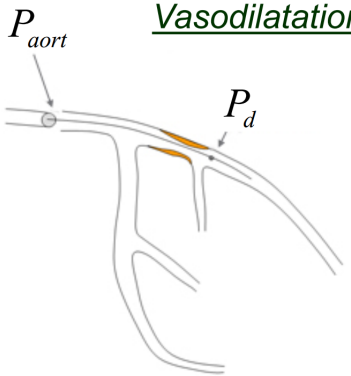

$$FFR = \frac{\text{pressure distal to the lesion } (P_d)}{\text{aortic pressure } (P_{aort})}$$

$FFR = 1 \longrightarrow$ healthy subject

$FFR \leq 0.75 \longrightarrow$ surgical treatment

Segmentation [7]

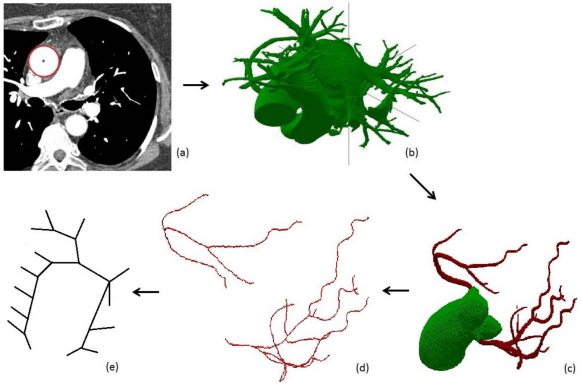

[7] Patient-specific anatomical models in human physiology. Rus. J. Num. Anal. Math. Mod. 30(3), 185–201 (2015)

Segmentation

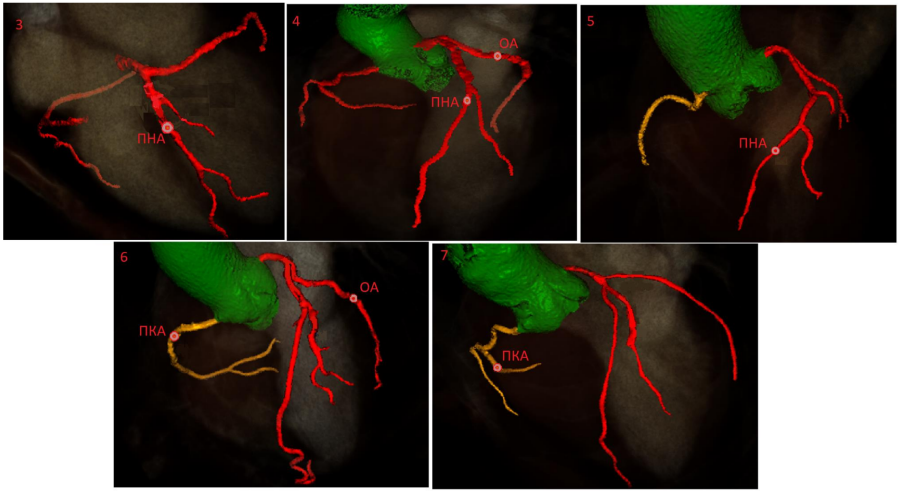

Attaching individual structure to the systemic arteries

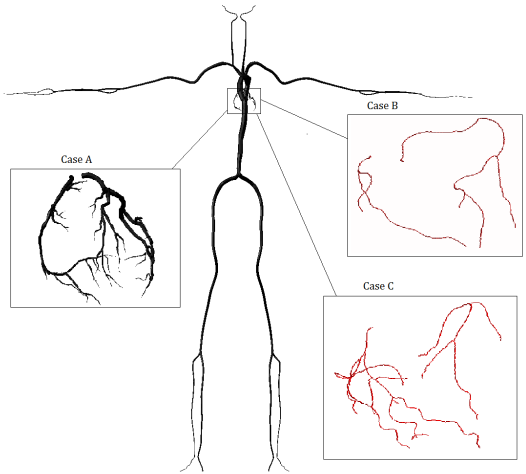

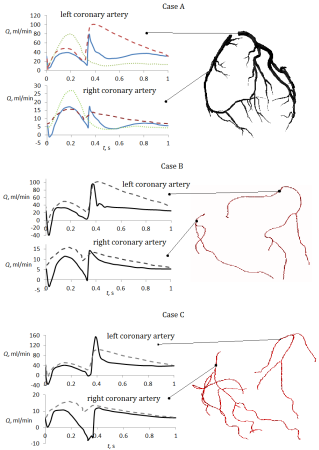

Fractional flow reserve [8]

Patient	Vessel	Stenosis	Length, mm	FFR	FFR model	Deviation
1	LAD	50%	40	0.58	0.51	14%
	LCA	55%	2	0.84	0.72	17%
	LCX	80%	10	0.61	0.59	3%
2	LAD	80%	20	0.78	0.74	5%
	RCA	55%	2	0.87	0.93	-5%
3	RCA	70%	20	0.77	0.81	-5%
4	RCA	60%	40	0.57	0.6	-5%
	LCX	50%	10	0.97	0.88	14%
5	LAD	50%	10	0.86	0.91	-5%
6	LCX	50%	10	0.83	0.89	-7%
	RCA	50%	10	0.93	0.91	2%
7	RCA	50%	3	0.89	0.85	5%

[8] Virtual fractional flow reserve assessment in patient-specific coronary networks by 1D hemoДинамические model. Rus. J. Num. Anal. Math. Mod. 30(5), 269–276 (2015)

Fractional flow reserve: benchmark (10 patients) [9]

- Pearson correlation coefficient ≈ 0.66, (moderate positive relationship).
- Mean absolute deviation $4.9 \cdot 10^{-2}$.
- Predicted values of FFR lay in 95% confidence interval.

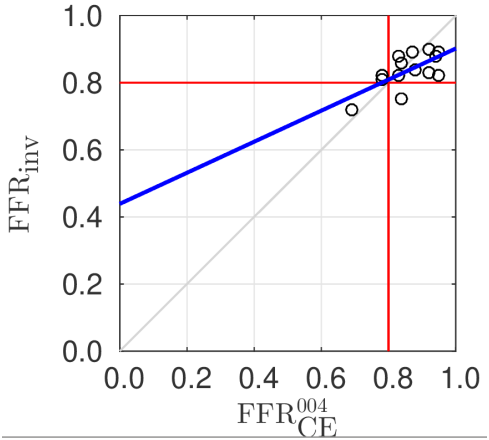

[9] Non-invasive coronary CT angiography-derived FFR: A benchmark study comparing the diagnostic performance of 4 computational methodologies. Int. J. of Num. Met. Biomed. Eng., 35(10), e3235 (2019)

Removing stenosis from carotid artery

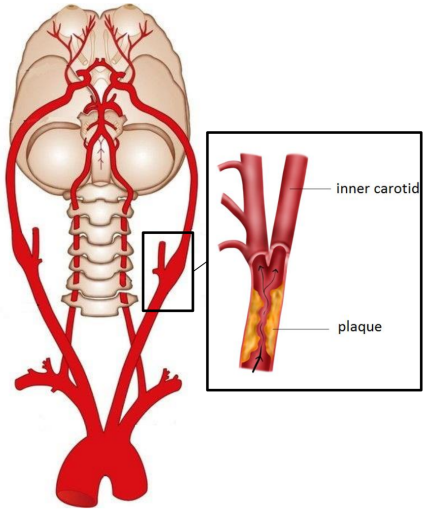

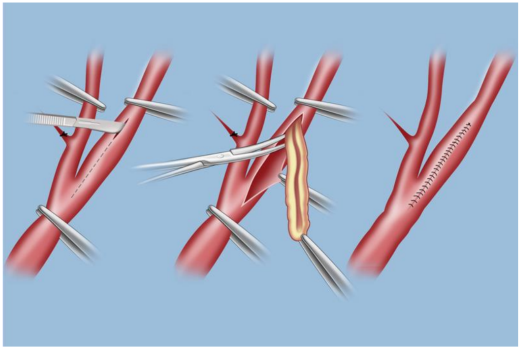

Patient-specific vascular network construction

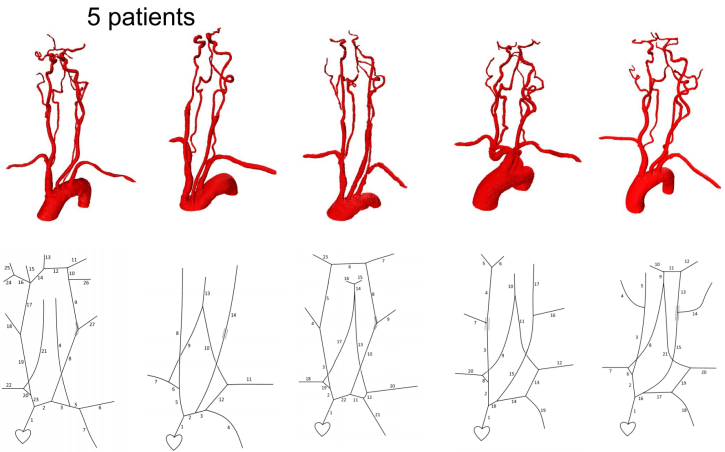

Ultrasound measuremetns of the linear velocities in control points

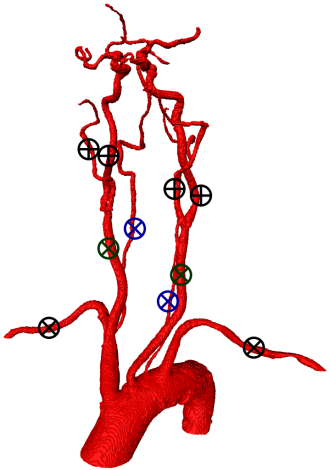

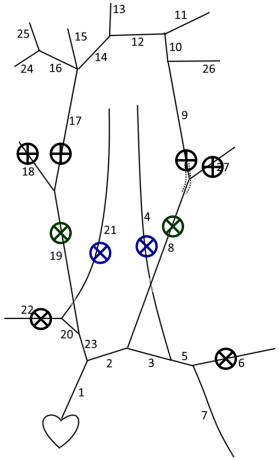

Stenosed regions detection

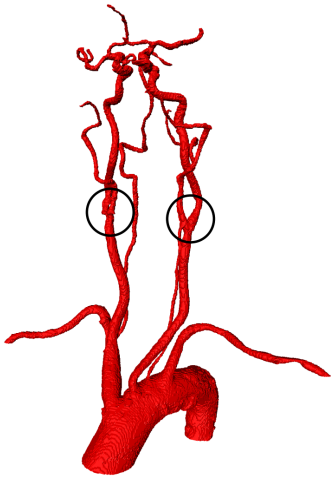

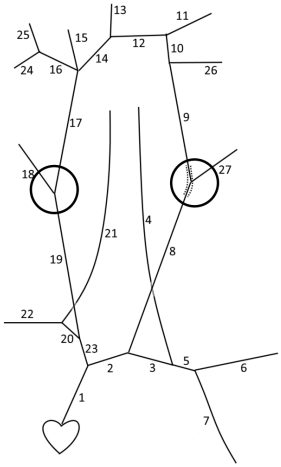

Stenosis

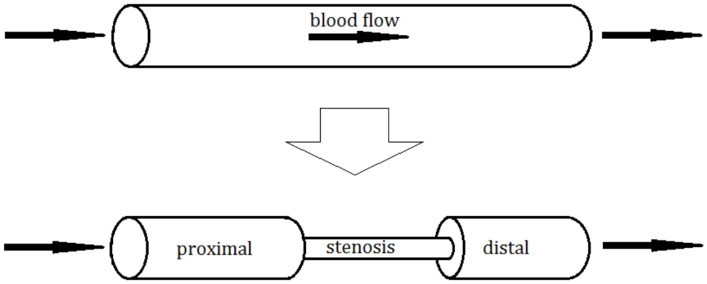

Modeling before sugery: unknow parameters identification (fitting) [10]

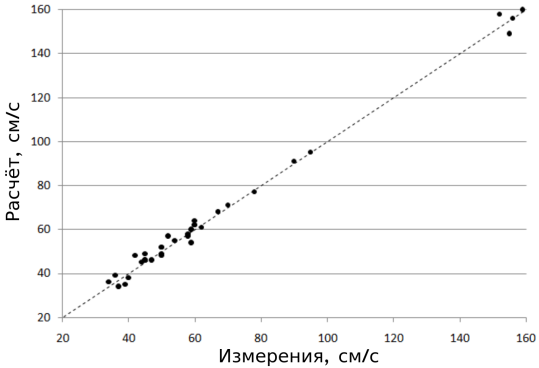

$$\bar{\sigma} = 2.2\%, \quad \sigma_{max} = 6\%$$

[10] Mathematical modelling of circulation in extracranial brachiocephalic arteries at pre-operation stage in carotid endarterectomy. Russian Journal of Cardiology, 144(4), 88–92, (2017)

Modeling after surgery: prediction [11]

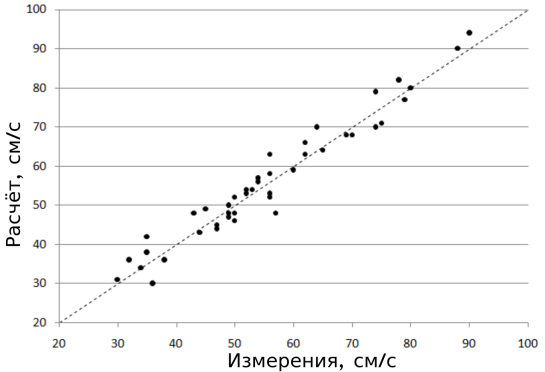

$$\bar{\sigma} = 3\%, \quad \sigma_{max} = 9\%$$

[11] Mathematical modelling of circulation in extracranial brachiocephalic arteries at pre-operation stage in carotid endarterectomy. Russian Journal of Cardiology, 144(4), 88–92, (2017)

Influence of Willis Circle to the cerebral blood flow during stenoses of carotid arteries

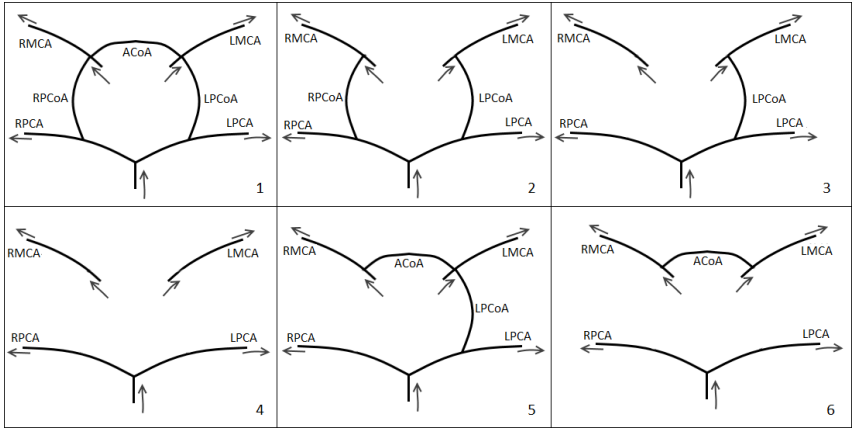

Case 1: full Circle of Willis

Stenoses	Blood flow, ml/s			
	LMCA	RMCA	LPCA	RPCA
no stenoses	1.20	1.21	0.45	0.43
LICA, RICA, LVA,RVA	0.23	0.23	0.09	0.08
RICA, LVA, RVA	1.19	1.20	0.44	0.43
LICA, RICA, LVA	1.17	1.18	0.44	0.43
LICA, RICA	1.20	1.20	0.44	0.43
LVA, RVA	1.20	1.20	0.44	0.43
LICA	1.20	1.20	0.45	0.43
LVA	1.20	1.20	0.45	0.43

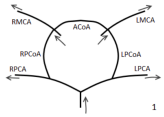

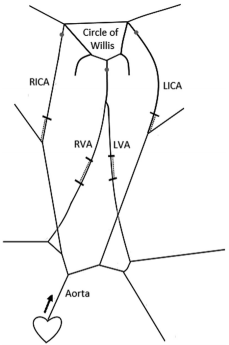

Case 6: Absense of RPCoA and LPCoA

Stenoses	Blood flow, ml/s			
	LMCA	RMCA	LPCA	RPCA
no stenoses	1.20	1.21	0.45	0.43
LICA, RICA, LVA,RVA	0.17	0.17	0.14	0.14
RICA, LVA, RVA	1.21	1.21	0.13	0.12
LICA, RICA, LVA	0.17	0.17	0.46	0.45
LICA, RICA	0.17	0.17	0.46	0.45
LVA, RVA	1.21	1.22	0.13	0.12
LICA	1.20	1.20	0.45	0.43
LVA	1.20	1.20	0.45	0.43

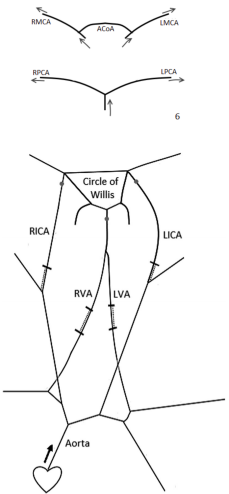

ELSEVIER

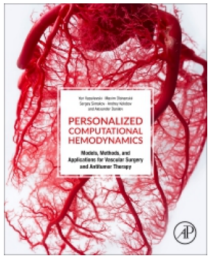

Personalized Computational Hemodynamics

1st Edition

Models, Methods, and Applications for Vascular Surgery and Antitumor Therapy

☆☆☆☆☆ Write a review

Authors: Yuri Vassilevski, Maxim Olshanskii, Sergey Simakov, Andrey Kolobov, Alexander Danilov

Paperback ISBN: 9780128156537

Imprint: Academic Press
Published Date: 27th April 2020